







New Possibilities of Creating the Efficient Dimensionally Stable Composite Honeycomb Structures for Space Applications

A. Kondratiev , V. Gaidachuk , T. Nabokina ,
and A. Tsaritsynskiy 

National Aerospace University Kharkiv Aviation Institute,
Chkalova Str., 17, Kharkiv 61070, Ukraine
a.kondratiev@khai.edu, tsaritsynskyy.a.a@gmail.com

Abstract. Today there is a great need in the optimal designing and manufacturing of dimensionally stable precision structures for satellite communication systems and sensing systems, in order to implement the international space programs successfully. It is well known that sandwich panels with load-bearing skins made of polymeric composites based on carbon, organic or glass fibers and honeycomb filler of aluminum foil or other materials providing combined action of skins, feature high dimensional stability. Optimization of design parameters was performed on a specimen of operating section of the composite solar panel with honeycomb filler. Results of the analysis of various reinforcement patterns for the load-bearing skins and rational distribution of material for several loading cases of the solar panel are presented. Technological warpage of these panels was analyzed and assessed. Causes of defects generated during the manufacturing process in the form of continuous and discrete strips of thin load-bearing skins of CFRP (carbon fiber reinforced plastic) were also investigated. With the use of the analytical methods supported by finite element method, the integrated study of the adhesive joint's bearing capacity of solar panel composite skins with the honeycomb filler at transverse avulsion for the main technological methods of applying the adhesive (as a continuous layer and targeted dosing to the ends of the honeycomb) was carried out. The results obtained allow predicting the fracture behavior of the load-bearing skins' bonding with the honeycomb filler depending on parameters and properties of the honeycomb cell material and the adhesive layer.

Keywords: Honeycomb structures · Optimal designing · Space applications

1 Introduction

At present time, the international space projects more actively employ the programs on launching new satellite communication systems and sensing systems into space. Creation of spacecrafts (SC) of new generation which put forward higher demands to quality, reliability and competitiveness in the global market of space services requires the development of new structural layouts (SL) or modernization of existing ones. It is also worth noting that speed of data transmission and accuracy of location of SC-serviced ground objects and near-to-Earth objects is increasing constantly.

Specific feature of structures operating in the conditions of open space and meant for precision coordination of SC relationship with ground objects is the necessity of meeting rather strict requirements including provision of thermal dimensional stability thereby [1].

It is known that high and stable stiffness is featured by sandwich structures with fillers of various types among which the honeycomb fillers are the most widely used in rocket and space technology (RST) [2]. Unique set of strength, technological and operational characteristics of such structures has shown their priority among other classes of sandwich structures and predetermined their extensive use in rocket and space technology [3].

A promising direction in the creation of precision honeycomb structures (HS) is using of polymeric composite materials (PCM) based on carbon fibers and polymeric matrices in such structures [4]. Necessity of continuous improvement of their efficiency promoted growth of theoretical and experimental investigations aimed at development of the methods of optimal designing of products of that class and creation of pilot-design units to be operated in the conditions of open space [5]. To a certain extent, it was promoted by the works of the team of contributors aimed at enhancing of the scientific support of creation of PCM honeycomb structures for RST results of which are summarized in monographs [6] and a number of our reports such as [7, 8].

2 Analysis of Various Bearing Skins' Reinforcement Patterns and Rational Distribution of Material of Solar Panel at Its Multiple-Factor Loading

Usually, solar panels are experiencing high overloads in the process of launch vehicle start, as well as vibration impacts and thermo-cycling. At optimal solar panel designing, with a view to meeting strict requirements asserted therefor it is necessary to obtain the most accurate values of parameters of stress-strain distribution (SSD) in its structural elements for the whole spectrum of external impacts specified.

Ample opportunities of the modern software systems implementing the finite element method (FEM) allow ensuring to the full extent and within reasonable time the targeted optimal designing of that class of structures [9].

The authors previously initiated the studies in this area, and by now the contours of the present-day concept of optimization of basic parameters of RST structures made of PCM are outlined [6]. Within the framework of this concept, implementing of comprehensive approach to creation of precision HS for space applications continues, and the essence of the above approach consists in:

- theoretical prediction of maximum possible reduction of surface mass of products at the current and future levels of the material and technical base;
- subsequent analysis of technological capabilities of manufacturing solar panels with minimal surface mass taking into account the progress of materials used;
- revealing typical defects associated with the prospective level of solar panel production, determining their potential risk for the normal functioning of products in service, and finding the ways to avoid it.

Below, by the example of the operating section of composite solar panel with the honeycomb filler (HF) the results of theoretical prediction of maximum possible reduction of surface mass of solar panel at multiple-factor loading thereof are given [6].

Geometrical parameters of SC solar panel are shown in Fig. 1.

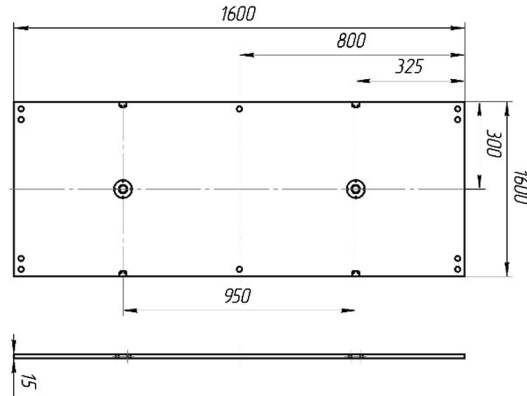


Fig. 1. Geometrical parameters of SC solar panel

Investigations were carried out as based on the requirements that the solar panel is to maintain its characteristics in the absence of mechanical damage after its exposure to:

- loads during acceptance tests by bending;
- quasi-static loads of the launch phase: longitudinal load of 15 g (along the longer side of the panel); lateral load of 10 g (along the shorter side and normally to the panel surface);
- acoustic loads;
- temperature field from minus 160 °C to plus 100 °C.

Calculation of SSD of solar panel was made with the use of software package of finite-element analysis. At its discretization to the finite element grid, four-unit multilayer shell-type finite element was used, with the bending and membrane properties. Base layers (BL) were simulated in the form of packages of the finite number of monolayers with the relevant physical and mechanical characteristics (PhMC). HF was represented as a conventional, uniform by volume layer of the finite element being used. Finite element model of the solar panel is represented by 10400 elements.

For evaluation of stress state of the base layer, Von-Mises–Hill energy failure criterion for layered PCM was used.

The diagrams of fixation and loading of the solar panel during acceptance tests, rated values of deflection, boundary conditions corresponding to them in the finite element analysis software system and examples of the patterns of strained state are represented in Fig. 2.

Below stated mass loads are adopted as quasi-static loads in the launch phase:

- longitudinal load of 15 g;
- lateral load of 10 g.

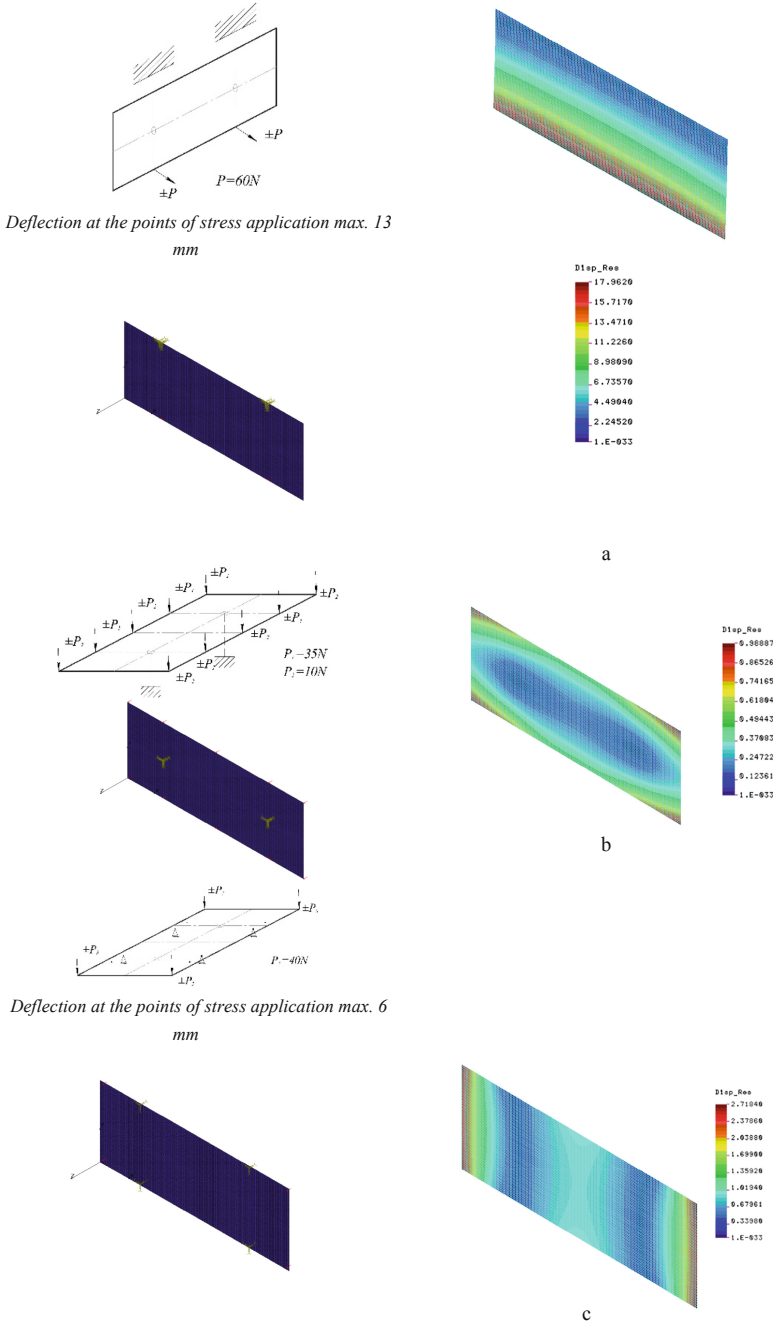


Fig. 2. Diagrams of static bending tests of the solar panel during acceptance tests, rated values of deflection, boundary conditions corresponding to them in the finite element analysis software system, patterns of strained state (mm)

Example of the result of calculation of the solar panel model under action of quasi-static loads is given in Fig. 3.

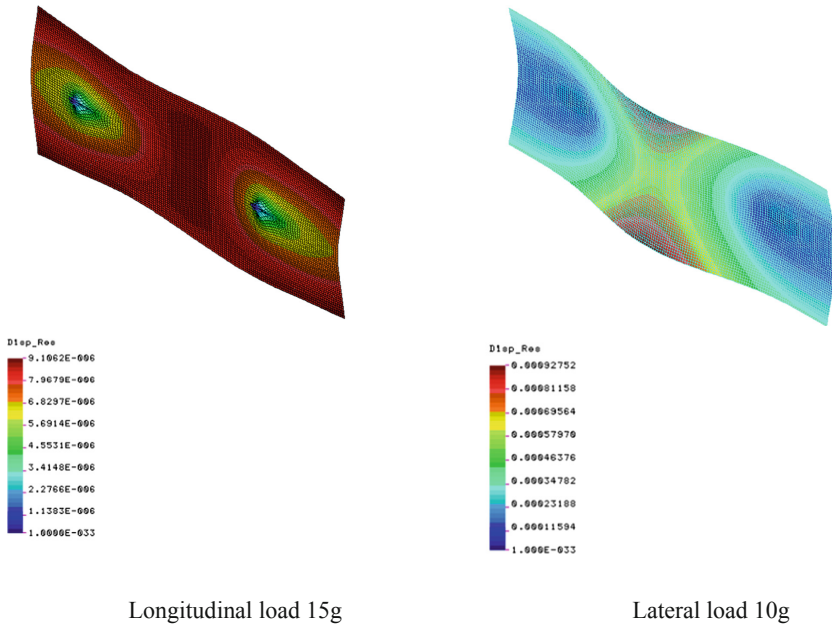


Fig. 3. Pattern of strained state of the solar panel under action of quasi-static loads (m)

Evaluation of solar panel acoustic strength was performed for the first three modes of its self-oscillations, results of calculations for which are given in Table 1.

Table 1. First three calculated self-oscillation modes for solar panel

Oscillation mode	Value
1	90,03 Hz
2	106,40 Hz
3	145,09 Hz

Taking into account that acoustic loads act on the solar panel in “closed” state when it is launched into orbit, we considered the supporting conditions similar to the second acceptance tests’ diagram (Fig. 2, b).

Under action of the variable acoustic loads (acoustic pressure), there occur forced oscillations with the continuous set of frequencies. Table 2 gives frequencies of forced oscillations close to obtained self-oscillation values of the solar panel, with the values of acoustic and amplitude pressures relevant thereto.

Table 2. Frequencies of forced oscillations of the solar panel close to the values of self-oscillations

Basic frequency of 1/3 octave band, Hz	Level of acoustic pressure (regarding $2 \cdot 10^{-5}$ Pa), dB	\bar{p} , Pa	p_{max} , Pa
80	132	79	112
100	133	89	126
125	134	100	141
160	135	112	159

To enable further evaluation of the effect of resonant phenomena, we calculated the solar panel model under action of maximum possible static pressure of the frequency range considered $p_{max} = 159$ Pa.

The given value corresponds to the acoustic pressure of 135 dB with the basic frequency of 1/3 octave band, 160 Hz. Figure 4 represents the results of calculations of the solar panel under action of static pressure of $p_{max} = 159$ Pa equivalent to the acoustic pressure of 135 dB with the basic frequency of 1/3 octave band, 160 Hz. For calculation of the solar panel model under action of the forced oscillations, we've carried out the dynamic harmonic analysis [6].

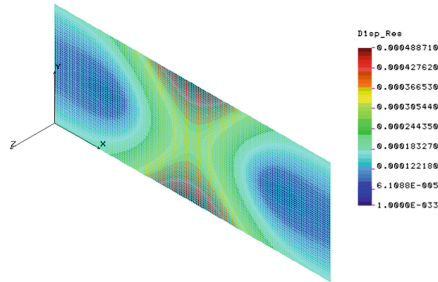


Fig. 4. Pattern of strained state of the panel under action of the static pressure thereon, equivalent to acoustic pressure of 135 dB

We have investigated the range of forced acoustic frequencies of 80..160 Hz which completely covered the range of the relevant self-frequencies of the solar panel model. Figure 5 shows the resulting graphic chart of the amplitude-frequency characteristics of the solar panel.

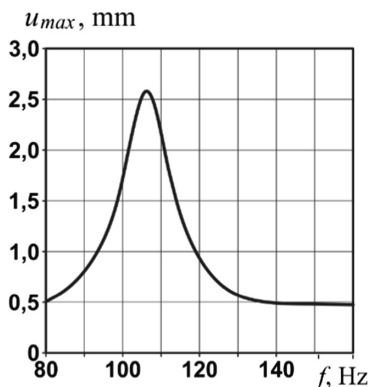


Fig. 5. Graphic chart of the amplitude-frequency characteristic for maximum resulting movement of the solar panel

Besides, the solar panel is exposed to the temperature impact. The range of temperatures is from minus 160 °C to plus 100 °C. It is evident that the given loading case is typical for the normal operation of the solar panel in the open space in its expanded state. This being the case, the temperature regime of the solar panel is stipulated by the mode of its operation: upper surface of the panel is heated since photo-converters are absorbing the solar energy, while the lower one is always in the shade.

With a view to evaluating the load-bearing capacity of the solar panel under action of maximal possible temperature drop thereon the relevant temperature gradient was found. Results of the calculation of solar panel model under action of the temperature gradient are shown in Fig. 6.

When searching for the rational distribution of the base layer material, two potential materials have been investigated: conventional carbon fiber of TAIRFUL type and high-modulus one Kulon P-VK36RT.

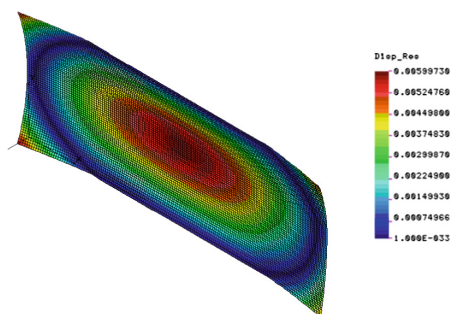


Fig. 6. Pattern of strained state of the solar panel under action of the temperature gradient thereon (temperature drop is from minus 160 to plus 100 °C)

As based on the technological capabilities of producing the carbon fibers of the above types, we considered a number of possible thicknesses of prepreg (mono-layer) in the range of: $t = 0,04 \dots 0,08$ mm. During the search of the rational distribution of the base layer material, a number of reinforcement patterns thereof were considered.

The rational parameters of reinforcement patterns of base layers of the solar panels were obtained by superimposition of zones of their use which are feasible by strength and stiffness. Obtained rational variants of the solar panel base layer reinforcement pattern are summarized in Table 3.

Table 3. Obtained rational parameters of the solar panel

Two layers for the base layer	
Kulon P-VK36RT	TAIRFUL
$t = 0,05$ mm; mass 0,5336 kg	$t = 0,07$ mm; mass 0,6488 kg
Reinforcement pattern	Reinforcement pattern
$\pm 60^\circ$	$\pm 60^\circ, -60^\circ$
Three layers for the base layer	
Kulon P-VK36RT	TAIRFUL
$t = 0,04$ mm; mass 0,5915 kg	$t = 0,05$ mm; mass 0,6773 kg
Reinforcement pattern	Reinforcement pattern
$0^\circ, \pm 75^\circ$	$0^\circ, 90^\circ, 90^\circ$

We have also considered possible methods of the rational distribution of material in the solar panel model:

- usage of advanced technological operations on decreasing the base layer thickness (flattening-out) or its discretization;
- choice of the structural layout providing for reinforcement between the embedded elements for mounting with the use of locks, hinge assemblies and stops.

The above results of the comparative analysis of the various options of reinforcement patterns and distribution of base layer material gave the reason to expect a possibility in principle to reduce the specific weight of the solar panel for the rated loading cases to the level of $0,6 \text{ kg/m}^2$.

However, provision of the minimal weight of solar panels at specified operating conditions is connected with a number of technological peculiarities and production problems not occurring with the creation of similar structures: possibility of formation of skins which thickness is comparable with thicknesses of elementary reinforcing fibers of PCM; provision of minimal application of adhesive during the panels' forming; development of the operating procedures of solar panels' production which ensure the specified quality and service life of products.

Analysis of continual and discrete contractions of thin base layers of solar panels

In the process of experimental investigations of the capabilities of making solar panels with thin base layers on the pilot models of solar panel fragments some

technological problems were revealed [6]. Typical defects for solar panels with thin base layers are as follows: uniformly distributed on the surface (continual) contractions of base layers (“rippled surface”) (Fig. 7) and considerable random discrete contractions of skins above individual cells of honeycombs (“dips”).

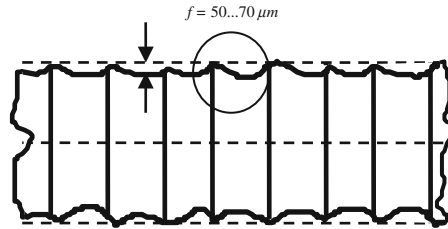


Fig. 7. Diagram of continual contractions of thin base layers of solar panels

Apart from these new defects, the known effect of technological warpage of the solar panel connected with the thermal instability of skins was revealed. Continual contractions of base layers of the solar panels were investigated on the basis of the mathematical model taking into account the kinetics of the process of skins-to-honeycomb bonding. Mathematical model was offered which took into account the thermal expansion of the base layer and honeycomb filler at the temperature of panel bonding, with the subsequent cooling-down and fixation of the adhesive in the heated state, and further cooling of the bonded panel to the normal temperature [6].

Solving of this task allowed obtaining the value of continual contraction of f depending on parameters varying in the process of bonding:

- shrinkage $\varepsilon^y(\tau)$:

$$\varepsilon_y(\tau) = \begin{cases} \varepsilon_{max}^y \cdot tg^n\left(\frac{\tau-\tau_0}{\tau_n}\right) & \text{at } \varepsilon_y \leq \varepsilon_{max}^y \\ \varepsilon_{max}^y & \text{at } \varepsilon_y > \varepsilon_{max}^y \end{cases} \quad (1)$$

- coefficient of linear thermal expansion (CLTE) of adhesive $\alpha(\tau)$:

$$\alpha(\tau) = \begin{cases} \alpha_c \left[0, 2 + \left(\frac{\tau}{\tau_n}\right)^{\ln\left(\frac{0.8}{0.7}\right)} \right] & \text{at } \alpha \leq \alpha_c \\ \alpha_c & \text{at } \alpha > \alpha_c \end{cases} \quad (2)$$

- adhesive elasticity modulus $E(\tau)$:

$$E(\tau) = \begin{cases} E_c \cdot \sqrt{\frac{\tau-\tau_2}{\tau_4}} & \text{at } E \leq E_c \\ E_c & \text{at } E > E_c \end{cases} \quad (3)$$

where τ - current time of polymerization process; τ_0 - incubation period from which the shrinkage starts ($\tau_0 = \tau_1$); τ_n - time of completion of intensive polymerization

($\tau_n = \tau_3$); $\tau^* > \tau_I + \tau_{II} + \tau_{III}$; τ_2 и τ_4 - time of completion of the second and fourth stages of bonding process, accordingly; ε_{max}^y , α_c , E_c - relevant parameters of cured adhesive; n - empiric constant depending on the rate of temperature rise.

Our calculations showed that taking the kinetics of adhesive curing into account leads to the considerable reduction of residual technological stresses in the solar panel.

It was established that the reason of discrete contractions of single cells of the solar panel is the absence of perforations at faces which results in occurrence of pressure difference (rarefaction) inside the defective cell and perforated cells surrounding it. On the basis of our investigations, the recommendations were given on reduction of deflections by means of the rational combination of technical capabilities to form the panel of thermally instable skins with the operating conditions thereof [6].

Analysis of possible reasons of occurrence of the technological warpage of solar panel in rather full scope forms the complex of engineering support of the given class of products' manufacturing.

3 Analysis of Load-Bearing Capacity of the Adhesive Joint of HS Base Layer

One of the deficiencies of honeycomb structures is the potential tear-off of the bearing skins from the honeycomb filler because of excessive pressure inside. There are various methods of application of the adhesive layer on skins: from the solution or melt onto ends of HF and by means of adhesive films [6]. Each of these methods provides for its own thickness of the adhesive layer which results in HS with the various surface mass. Optimization of the adhesive layer thickness is one of the ways of weight improvement of the RST honeycomb structures. However, less adhesive applied causes reduction of the load-bearing capacity of the product as well. Therefore, there is an urgent need to solve the task of determining the load-bearing capacity of the adhesive joint of HS skins at transversal tear-off for the basic technological methods of adhesive application. In the process of making the HF with BL using liquid or film-forming adhesive of η_{ad} thick, depending on the pressure of panel forming there is varying relative depth of penetration of ends of HF faces into the adhesive film $\bar{\eta} = \eta^*/\eta_{ad}$ (Fig. 8).

When considering the typical element of the honeycomb block with the cell of irregular hexagonal shape (Fig. 9) it was found that failure of the joint on foil would occur with fulfillment of in equation:

$$\frac{p_t a_c K (K \cos \beta + 1) \sin \beta}{(K + 1) \delta_c} \leq \sigma_{vmax}, \quad (4)$$

where p_t - pressure at transversal tear-off.

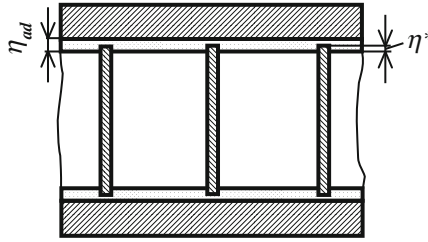


Fig. 8. Version of HF with BL bonding with the use of adhesive film

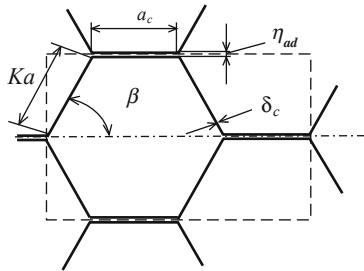


Fig. 9. Typical element of honeycomb block

For determining of load-bearing capacity of the joint on the adhesive finite-element model was used. Investigations were carried out for the plain strain at stresses in the aluminium foil of $\sigma_g=1$ MPa of $\delta_c = 30 \mu\text{m}$ thick with the elasticity modulus of $E_f = 70$ GPa at Poisson ratios of the foil and adhesive $\mu_f = \mu_\eta = 0,3$ for adhesives with elasticity moduli of $E_{\eta_1} = 3,5$ GPa, $E_{\eta_2} = 7$ GPa and $E_{\eta_3} = 15,6$ GPa and thicknesses of the adhesive layer of $\eta_1 = 0,05$ mm, $\eta_2 = 0,12$ mm and $\eta_3 = 0,2$ mm.

An example of the pattern of strained state of the finite-element model of the fragment of honeycomb block typical element at depth of penetration of HF faces' ends $\bar{\eta}^* = 0,7$ is shown in. Figure 10.

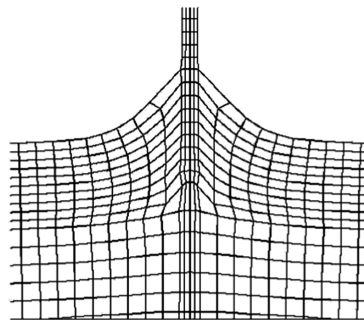


Fig. 10. Example of strained state of the model of honeycomb block typical element's fragment

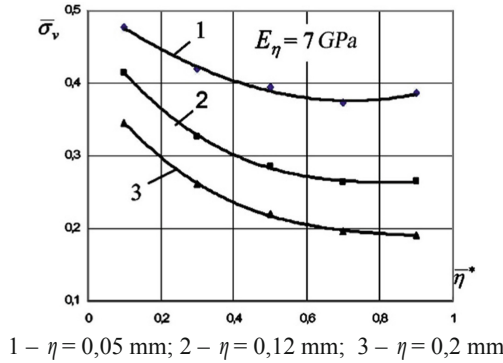


Fig. 11. Graph of variance of the relative maximum equivalent stresses on the relative depth of the gap

Figure 11 shows the graphs of variance of the relative maximum equivalent stresses on the relative depth of the gap for the adhesive elasticity modulus $E_\eta = 7 \text{ GPa}$.

Using similar method, investigations for the honeycombs of Nomex polymeric paper were carried out [6]. We have found the distinguishing features of behavior of adhesive joints with aluminium foil and Nomex polymeric paper under the load which are to be taken into account in designing and manufacturing HS.

One of the ways of the further reduction of HS surface mass is the implementation of technology of targeted dozed application of adhesive onto ends of honeycombs, which excludes its passive weight filling the inter-cell surface, not involved in ensuring the load-bearing capacity of the adhesive joint at transversal tear-off of the base layers [6]. We have carried out the analysis of analytical and finite-element methods of evaluation of the HS bearing capacity at transversal tear-off for the case of targeted dozed application of adhesive onto ends of HF faces (Fig. 12).

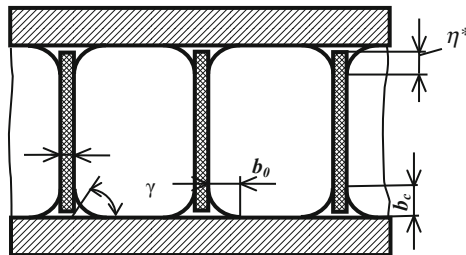


Fig. 12. Bonding of HF with skins of sandwich type with the use of adhesive applied onto ends

In the analytical solution we obtained the formula for medium equivalent stresses in the adhesive leg

$$\sigma_{vmax} = \frac{a_s K (K \cos \beta + 1) \sin(\beta) p_{an} (\xi_{\sigma,\mu}^2 + tg^2 \gamma) \sqrt{\cos^2 \gamma + 3 \sin^2 \gamma}}{2(K+1)b_0 \xi_{\sigma,\mu} \sqrt{1 + tg^2 \gamma} (\xi_{\sigma,\mu} + tg \gamma - \sqrt{2 \xi_{\sigma,\mu} tg \gamma})}$$

where $\xi_{\sigma,\mu} = b_c/b_0$ depends on parameters of surface tension at the boundary of adhesive with BL and material of honeycombs, viscosity of the adhesive and parameters of wetting of the interface.

Figure 13 shows the pattern of distribution of equivalent stresses in the adhesive fillet obtained on the basis of the finite-element model, and Fig. 14 gives the comparison of results of calculation of relative maximum equivalent stresses on both of these two models.

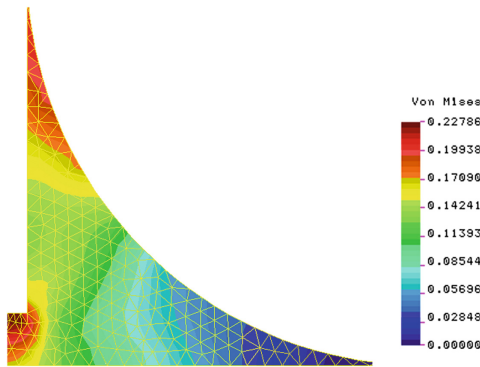


Fig. 13. Pattern of distribution of equivalent stresses in the adhesive fillet obtained on the basis of the finite-element model

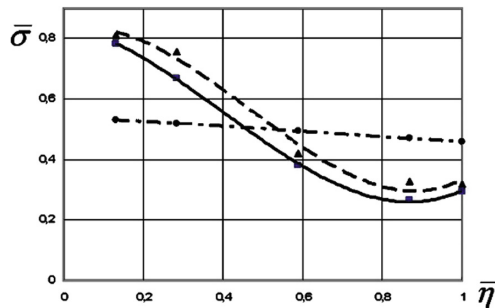


Fig. 14. Dependence $\bar{\sigma}_v = f(\bar{\eta})$ for various adhesives at: — $E_{\eta} = 15,6$ GPa; - - $E_{\eta} = 7$ GPa; — · — analytical dependence

As it is seen from graphs, analytical model gives the result agreeing with the result of the finite-element model only with the relative depth of penetration of honeycomb

ends into adhesive equal to 0,5. The finite-element model is also sensitive to the modulus of adhesive elasticity which influence, evidently, is not significant.

On the basis of results of the analysis it is concluded that bonding of skins with honeycombs is recommended to be performed at temperature of the forming pressure which ensures the relative depth of penetration of honeycomb ends into adhesive exceeding 0,5.

4 Conclusions

1. Theoretical prediction of the maximum possible reduction of the surface mass of composite solar panel with the honeycomb filler gave the reason to rely on the possibility in principle to reach its surface mass within the limits of 0,55... 0,6 kg/m².
2. We have established the rational diagrams of BL reinforcement of two and three mono-layers of solar panels of PCM based on carbon fibers TAIRFUL and Kulon P-VK36 RT with honeycomb fillers featuring various cell size which provide for minimal weight thereof.
3. We have developed the mathematical models of forming continual and discrete contractions of thin base layers of the solar panels in the process of their bonding with the honeycomb filler, on the basis of which analytical dependencies for determination of maximal depth of contractions are obtained.
4. The method of analysis of honeycomb structures' load-bearing capacity at transversal load is offered, allowing predicting with the reasonable accuracy the nature of their failure depending on parameters of HF cell, adhesive layer, PhMC and strength of the adhesive for specified temperature and pressure of bonding which determine one or another relative depth of penetration of HF faces' ends into the adhesive layer. Therefore, the above results in a complex form a scientific basis for the creation of modern and promising solar panels and can be used in manufacturing of the other precision products for space and conversion applications.

References

1. Webb, G., Da Silva Curiel, A.: Is access to space really a hurdle? Proceedings of the International Astronautical Congress, IAC 59, Glasgow, United Kingdom, 28 September–3 October 2008. *Our World Needs Space*, vol. 7, pp. 4064–4077 (2008)
2. Nunes, J.P., Silva, J.F.: Sandwiched composites in aerospace engineering. In: *Advanced Composite Materials for Aerospace Engineering*, pp. 129–174 (2016)
3. Herrmann, A.S.: *Design and Manufacture of Monolithic Sandwich Structures with Cellular Cares*, 274 p. Technomic Publishing Company, Stockholm (1999)
4. Slyvynskiy, V.I., Alyamovskiy, A.I., Kondratjev, A.V., Kharchenko, M.E.: Carbon honeycomb plastic as light-weight and durable structural material. In: *63rd International Astronautical Congress, IAC 2012*, vol. 8, pp. 6519 – 6529. Curran, Red Hook (2012)
5. Ganguli, R.: Optimal design of composite structures: a historical review. *J. Indian Inst. Sci.* **93** (4), 557–570 (2013)

6. Gaydachuk, A.V., Karpikova, O.A., Kondratiev, A.V., Slivinskiy, M.V.: Sotovyie zapolniteli i panelnyie konstruksii kosmicheskogo naznacheniya. Tehnologicheskie nesovershenstva sotovyih zapolniteley i konstruksiy, p. 279. National Aerospace University Kharkiv Aviation Institute Publ., Kharkiv (2012). ISBN 978-966-662-273-3
7. Kondratiev, A., Gaidachuk, V.: Weight-based optimization of sandwich shelled composite structures with a honeycomb filler. *East.-Eur. J. Enterp. Technol.* **1/1**(97), 24–33 (2019). <https://doi.org/10.15587/1729-4061.2019.154928>
8. Slyvynskiy, V.I., Sanin, A.F., Kharchenko, M.E., Kondratyev, A.V.: Thermally and dimensionally stable structures of carbon-carbon laminated composites for space applications. In: *Proceedings of the International Astronautical Congress, Our World Needs Space*, vol. 8, pp. 5739–5751 (2014)
9. Mackerle, J.: Finite element analyses of sandwich structures: a bibliography (1980–2001). *Eng. Comput.* **19**(2), 206–245 (2002). <https://doi.org/10.2514/2.991>